

# ALTERNATING PROJECTIONS GRIDLESS COVARIANCE-BASED ESTIMATION FOR DOA

Yongsung Park, Peter Gerstoft

Scripps Institution of Oceanography, University of California San Diego, La Jolla, CA, 92093-0238

## ABSTRACT

We present a gridless sparse iterative covariance-based estimation method based on alternating projections for direction-of-arrival (DOA) estimation. The gridless DOA estimation is formulated in the reconstruction of Toeplitz-structured low rank matrix, and is solved efficiently with alternating projections. The method improves resolution by achieving sparsity, deals with single-snapshot data and coherent arrivals, and, with co-prime arrays, estimates more DOAs than the number of sensors. We evaluate the proposed method using simulation results focusing on co-prime arrays.

**Index Terms**— DOA estimation, sparse signal recovery, off-grid sparse model, alternating projections, compressive sensing

## 1. INTRODUCTION

Direction-of-arrival (DOA) estimation is localizing several sources arriving at an array of sensors. It is an important problem in a wide range of applications, including radar, sonar, etc. Compressive sensing (CS) based DOA estimation, which promotes sparse solutions, has advantages over traditional DOA estimation methods. [1, 2] DOAs exist on a continuous angular domain, and gridless CS can be employed. [3, 4, 5] We propose a gridless sparsity-promoting DOA estimation method and apply it to co-prime arrays, which can resolve more sources than the number of sensors.

CS-based DOA estimation exploits the framework of CS, which promotes sparse solutions, for DOA estimation and has a high-resolution capability, deals with single-snapshot data, and performs well with coherent arrivals. [2, 3] To estimate DOAs in a continuous angular domain, non-linear estimation of the DOAs is linearized by using a discretized angular-search grid of potential DOAs (“steering vectors”). Grid-based CS has a basis mismatch problem [6, 7] when true DOAs do not fall on the angular-search grid. To overcome the basis mismatch, gridless CS [8, 9] has been utilized for DOA estimation. [3, 4, 5, 10, 11]

Gridless SPICE (GLS) [5, 12], one of the off-grid sparse methods, is a gridless version of sparse iterative covariance-based estimation (SPICE) [13]. GLS re-parameterizes the

data covariance, or sample covariance matrix (SCM), using a positive semi-definite (PSD) Toeplitz matrix, and finds the lowest rank Toeplitz matrix which fits the SCM. The Toeplitz-structured SCM is related to a Fourier-series, which is composed of harmonics. [14, 15] GLS-based DOA estimation retrieves DOA-dependent harmonics from the SCM parameter. [5] The GLS solver uses a semi-definite programming problem (SDP), which is infeasible in practice for high-dimensional problems.

Alternating projections (AP) algorithm [16, 17] has been introduced to solve matrix completion [18, 19, 20, 21] and structured low rank matrix recovery [22, 23] and consists of projecting a matrix onto the intersection of a linear subspace and a nonconvex manifold. Atomic norm minimization (ANM) [6, 8] solves gridless CS and is equivalent to a recovery of a Toeplitz-structured low rank matrix [24]. AP based on ANM has been applied to gridless CS for DOA estimation. [25, 26]

We propose AP-based GLS for gridless CS for DOA estimation. GLS reconstructs a DOA-dependent SCM matrix, which is a Toeplitz-structured low rank matrix and has a PSD matrix in its constraint. AP-GLS solves the reconstruction of the Toeplitz-structured low rank matrix by using a sequence of projections onto the following sets: Toeplitz set, rank-constraint set, and PSD set.

Co-prime arrays are introduced for DOA estimation and offer the capability of identifying more sources than the number of sensors. [27] Sparse Bayesian learning (SBL) deals with co-prime arrays without constructing a co-array based covariance matrix and shows accurate DOAs identifying more sources than the number of sensors. [28, 29] We apply AP-GLS to co-prime arrays and show that AP-GLS with co-prime arrays estimates more DOAs than the number of sensors.

We study the performance of AP-GLS with co-prime arrays for single- and multiple-snapshot data, incoherent and coherent sources, and when the number of sources exceeds the number of sensors.

## 2. SIGNAL MODEL AND CO-PRIME ARRAY

### 2.1. Signal model

We consider  $K$  narrowband sources for  $L$  snapshot data with complex signal amplitude  $s_{k,l} \in \mathbb{C}$ ,  $k = 1, \dots, K$ ,  $l = 1, \dots, L$ . The sources have stationary DOAs for  $L$  snapshots

Supported by the Office of Naval Research, Grant No. N00014-18-1-2118.

$\theta_k \in \Theta \triangleq [-90^\circ, 90^\circ]$ ,  $k = 1, \dots, K$  in the far-field of a linear array with  $M$  sensors. The observed data  $\mathbf{Y} \in \mathbb{C}^{M \times L}$  is modeled as

$$\mathbf{Y} = \sum_{k=1}^K \mathbf{a}(\theta_k) \mathbf{s}_{k:} + \mathbf{E} = \sum_{k=1}^K c_k \mathbf{a}(\theta_k) \boldsymbol{\phi}_{k:} + \mathbf{E}, \quad (1)$$

where  $\mathbf{s}_{k:} = [s_{k,1} \dots s_{k,L}] \in \mathbb{C}^{1 \times L}$ ,  $c_k = \|\mathbf{s}_{k:}\|_2 > 0$ ,  $\boldsymbol{\phi}_{k:} = c_k^{-1} \mathbf{s}_{k:} \in \mathbb{C}^{1 \times L}$  with  $\|\boldsymbol{\phi}_{k:}\|_2 = 1$ ,  $\mathbf{E} \in \mathbb{C}^{M \times L}$  is the measurement noise, and  $\mathbf{a}(\theta_k) \in \mathbb{C}^M$  is the steering vector. The steering vector is given by ( $\lambda$  is the signal wavelength and  $d_m$  is the distance from sensor 1 to sensor  $m$ )

$$\mathbf{a}(\theta_k) = \left[ 1 e^{-j \frac{2\pi}{\lambda} d_2 \sin \theta_k} \dots e^{-j \frac{2\pi}{\lambda} d_M \sin \theta_k} \right]^T. \quad (2)$$

## 2.2. Co-prime array

Consider the sensor positions in an array is given by  $d_m = \delta_m d$ ,  $m = 1, \dots, M$ , where the integer  $\delta_m$  is the normalized sensor location of  $m$ th sensor and  $d$  is the minimum sensor spacing. A uniform linear array (ULA) is composed of uniformly spaced sensors with  $\boldsymbol{\delta} = [0 \ 1 \dots M-1]^T$  and  $d = \lambda/2$ .

A co-prime array involves two ULAs with spacing  $M_1 d$  and  $M_2 d$  where  $M_1$  and  $M_2$  are co-prime, i.e., their greatest common divisor is 1. [27] A co-prime array consists of a ULA with  $\boldsymbol{\delta} = [0 \ M_2 \dots (M_1 - 1)M_2]^T$  and a ULA with  $\boldsymbol{\delta} = [M_1 \ 2M_1 \dots (2M_2 - 1)M_1]^T$ , a total of  $M_1 + 2M_2 - 1$  sensors.

We used a 16-sensor ULA with  $\boldsymbol{\delta} = [0 \ 1 \dots 15]^T$  and a 8-sensor co-prime array with  $M_1 = 5$  and  $M_2 = 2$ , i.e.,  $\boldsymbol{\delta} = [0 \ 2 \ 4 \ 5 \ 6 \ 8 \ 10 \ 15]^T$ .

## 3. ALTERNATING PROJECTIONS GRIDLESS SPICE

Consider the ULA case and assume incoherent sources. (GLS is robust to source correlations. [5, 12, 13]) In the noiseless case, the SCM  $\mathbf{R}^* \in \mathbb{C}^{M \times M}$  is given by

$$\mathbf{R}^* = \frac{1}{L} \mathbf{Y}^* \mathbf{Y}^{*H} = \sum_{k=1}^K p_k \mathbf{a}(\theta_k) \mathbf{a}^H(\theta_k) \quad (3)$$

where  $\mathbf{Y}^*$  is noise-free data and  $p_k > 0$ ,  $k = 1, \dots, K$  is the power of sources, i.e.,  $p_k = c_k^2$ . The SCM  $\mathbf{R}^*$  is a (Hermitian) Toeplitz matrix,

$$\mathbf{R}^* = \text{Toep}(\mathbf{r}) = \begin{bmatrix} r_1 & r_2 & \dots & r_M \\ r_2^H & r_1 & \dots & r_{M-1} \\ \vdots & \vdots & \ddots & \vdots \\ r_M^H & r_{M-1}^H & \dots & r_1 \end{bmatrix}, \quad (4)$$

where  $\mathbf{r} \in \mathbb{C}^M$ . Moreover,  $\mathbf{R}^*$  is PSD and has rank  $K$ . A PSD Toeplitz matrix of rank  $K < M$  can be uniquely decomposed (Vandermonde decomposition) [5, 6, 30] as

$$\mathbf{R}^* = \sum_{k=1}^K p_k \mathbf{a}(\theta_k) \mathbf{a}^H(\theta_k) = \mathbf{A} \text{diag}(\mathbf{p}) \mathbf{A}^H, \quad (5)$$

where  $\mathbf{A} = [\mathbf{a}(\theta_1) \dots \mathbf{a}(\theta_K)] \in \mathbb{C}^{M \times K}$ .

GLS uses a SCM-related parameter  $\mathbf{R} \in \mathbb{C}^{M \times M}$ , which is a rank- $K$  PSD Toeplitz matrix, and fits the parameter  $\mathbf{R}$  to SCM  $\tilde{\mathbf{R}} = \mathbf{Y} \mathbf{Y}^H / L \in \mathbb{C}^{M \times M}$ . The covariance fitting is implemented, in the case of  $L \geq M$  whenever  $\tilde{\mathbf{R}}$  is non-singular, by minimizing the criterion, [5, 12, 13]

$$\left\| \mathbf{R}^{-\frac{1}{2}} \left( \tilde{\mathbf{R}} - \mathbf{R} \right) \tilde{\mathbf{R}}^{-\frac{1}{2}} \right\|_{\text{F}}^2. \quad (6)$$

In the case of  $L < M$ , when  $\tilde{\mathbf{R}}$  is singular, the following criterion is used instead, [5, 12]

$$\left\| \mathbf{R}^{-\frac{1}{2}} \left( \tilde{\mathbf{R}} - \mathbf{R} \right) \right\|_{\text{F}}^2 = \text{tr}(\tilde{\mathbf{R}} \mathbf{R}^{-1} \tilde{\mathbf{R}}) + \text{tr}(\mathbf{R}) - 2 \text{tr}(\tilde{\mathbf{R}}). \quad (7)$$

GLS is achieved using the following optimization,

$$\begin{aligned} & \min_{\mathbf{R}} \text{tr}(\tilde{\mathbf{R}} \mathbf{R}^{-1} \tilde{\mathbf{R}}) + \text{tr}(\mathbf{R}) \quad \text{subject to } \mathbf{R} \succeq 0 \\ & \Leftrightarrow \min_{\mathbf{R}, \mathbf{Z}} \text{tr}(\mathbf{Z}) + \text{tr}(\mathbf{R}) \quad \text{subject to } \begin{cases} \mathbf{R} \succeq 0 \\ \mathbf{Z} \succeq \tilde{\mathbf{R}} \mathbf{R}^{-1} \tilde{\mathbf{R}}, \end{cases} \\ & \Leftrightarrow \min_{\mathbf{R}, \mathbf{Z}} \text{tr}(\mathbf{Z}) + \text{tr}(\mathbf{R}) \quad \text{subject to } \begin{bmatrix} \mathbf{R} & \tilde{\mathbf{R}} \\ \tilde{\mathbf{R}} & \mathbf{Z} \end{bmatrix} \succeq 0, \end{aligned} \quad (8)$$

where  $\mathbf{R} \succeq 0$  denotes  $\mathbf{R}$  is a PSD matrix and  $\mathbf{Z} \in \mathbb{C}^{M \times M}$  is a free variable. Consider the case of  $\mathbf{R} = \mathbf{R}^*$ , then  $\text{tr}(\mathbf{R}) = M \sum_{k=1}^K p_k$ . Defining  $\text{tr}(\mathbf{Z}) = M \sum_{k=1}^K p_k$ , the objective in (8), divided by  $2M$ , equals,

$$\frac{1}{2M} \text{tr}(\mathbf{R}) + \frac{1}{2M} \text{tr}(\mathbf{Z}) = \sum_{k=1}^K p_k. \quad (9)$$

Note that, in ANM, [6, 8] minimizing  $\sum_{k=1}^K p_k = \sum_{k=1}^K c_k^2$  is equivalent to minimizing the atomic norm,

$$\|\mathbf{Y}^*\|_{\mathcal{A}} = \inf_{c_k, \theta_k, \boldsymbol{\phi}_{k:}} \left\{ \sum_{k=1}^K c_k : \mathbf{Y}^* = \sum_{k=1}^K c_k \mathbf{a}(\theta_k) \boldsymbol{\phi}_{k:} \right\}. \quad (10)$$

The atomic norm is a convex relaxation of the atomic  $l_0$  norm, [6]

$$\|\mathbf{Y}^*\|_{\mathcal{A},0} = \inf_{c_k, \theta_k, \boldsymbol{\phi}_{k:}} \left\{ K : \mathbf{Y}^* = \sum_{k=1}^K c_k \mathbf{a}(\theta_k) \boldsymbol{\phi}_{k:} \right\}. \quad (11)$$

Minimizing the atomic  $l_0$  norm is equivalent to minimizing rank of  $\mathbf{R}^* = \mathbf{Y}^* \mathbf{Y}^{*H} / L$ . [5, 6] Summarizing, the term  $\text{tr}(\mathbf{R}) = \sum_{k=1}^K p_k$  is the nuclear norm, used as a convex relaxation of  $\text{rank}(\mathbf{R})$ .

By using the rank minimization in (8), the resulting optimization is as follows,

$$\min_{\mathbf{R}, \mathbf{Z}} \text{rank}(\mathbf{R}) \quad \text{subject to } \begin{bmatrix} \mathbf{R} & \tilde{\mathbf{R}} \\ \tilde{\mathbf{R}} & \mathbf{Z} \end{bmatrix} \succeq 0. \quad (12)$$

For the coprime array, we use the row-selection matrix  $\Gamma_\Omega \in \{0, 1\}^{M \times M_\Omega}$ , i.e.,

$$\mathbf{Y}_\Omega = \Gamma_\Omega \mathbf{Y} \text{ or } \mathbf{Y} = \Gamma_\Omega^\dagger \mathbf{Y}_\Omega, \quad (13)$$

where  $\mathbf{Y}$  is data of full  $M$ -element ULA and the Moore-Penrose pseudo-inverse  $\Gamma_\Omega^\dagger$ . The optimization for the coprime array is given as,

$$\min_{\mathbf{R}, \mathbf{Z}} \text{rank}(\mathbf{R}) \quad \text{subject to} \quad \begin{bmatrix} \mathbf{R}_\Omega & \tilde{\mathbf{R}}_\Omega \\ \tilde{\mathbf{R}}_\Omega & \mathbf{Z} \end{bmatrix} \succeq 0, \quad (14)$$

where  $\tilde{\mathbf{R}}_\Omega = \mathbf{Y}_\Omega \mathbf{Y}_\Omega^H / L \in \mathbb{C}^{M_\Omega \times M_\Omega}$  and  $\mathbf{R}_\Omega = \Gamma_\Omega \mathbf{R} \Gamma_\Omega^T \in \mathbb{C}^{M_\Omega \times M_\Omega}$ . To minimize  $\text{rank}(\mathbf{R})$ ,  $\mathbf{R}$  is calculated,

$$\mathbf{R} = \Gamma_\Omega^\dagger \mathbf{R}_\Omega (\Gamma_\Omega^\dagger)^T. \quad (15)$$

#### 4. ALTERNATING PROJECTIONS

We suggest alternating projections to reconstruct Toeplitz-structured low rank matrix in (12) and (14). AP-GLS involves the following sets: Toeplitz set, positive semi-definite (PSD) set, and rank-constraint set.

##### 4.1. Projection onto the Toeplitz set

The SCM-related parameter  $\mathbf{R}$  is a Toeplitz matrix, and the projection of  $\mathbf{R}$  onto the Toeplitz set  $\mathcal{T}$  is implemented by finding the closest Toeplitz matrix, [22, 31]

$$P_{\mathcal{T}}(\mathbf{R}) = \text{Toep}(\mathbf{r}), \quad (16)$$

$$r_m = \frac{1}{2(M-m)} \sum_{i=1}^{M-m} R_{i,i+m-1} + R_{i+m-1,i}^H. \quad (17)$$

Note that,  $m$ th component of  $\mathbf{r} \in \mathbb{C}^M$  is obtained by averaging  $m$ th diagonal and the conjugate diagonal components.

##### 4.2. Projection onto the PSD set

The constraints (12) and (14) include PSD matrices, which is obtained by projecting the matrix in the constraint onto the PSD set  $\mathcal{P}$ , defined by the PSD cone. The projection of a (Hermitian) matrix  $\mathbf{S}$  onto the PSD set is achieved from the eigen-decomposition  $\mathbf{S} = \sum_{i=1}^{2M} \mu_i \mathbf{q}_i \mathbf{q}_i^H$ , [16, 17]

$$P_{\mathcal{P}}(\mathbf{S}) = \sum_{i=1}^{2M} \max\{0, \mu_i\} \mathbf{q}_i \mathbf{q}_i^H. \quad (18)$$

##### 4.3. Projection onto the rank-constraint set

The objectives (12) and (14) include rank-constraints. Consider the case of rank- $K$  matrix  $\mathbf{R}$ . The projection of  $\mathbf{R}$  onto the rank-constraint set  $\mathcal{R}$  is achieved from the singular value decomposition and taking the  $K$ -largest singular values, [19, 23]

$$P_{\mathcal{R}}(\mathbf{R}) = \sum_{k=1}^K \sigma_k \mathbf{u}_k \mathbf{v}_k^H, \quad (19)$$

where  $\sigma_k$ ,  $\mathbf{u}_k \in \mathbb{C}^M$ ,  $\mathbf{v}_k \in \mathbb{C}^M$ ,  $k = 1, \dots, K$ , are the  $K$ -largest singular values and the corresponding left and right singular vectors. We remark that  $\mathbf{R}$  is an SCM, thus the eigen-decomposition and the singular value decomposition result in the same results.

---

#### Algorithm 1 AP-GLS

---

- 1: Input:  $\mathbf{Y} \in \mathbb{C}^{M \times L}$ ,  $K$ ,  $\Gamma_\Omega$
  - 2: Parameters:  $\epsilon_{\min} = 10^{-3}$
  - 3: Initialization:  $\mathbf{R} \in \mathbb{C}^{M \times M}$ ,  $\mathbf{Z} \in \mathbb{C}^{M \times M}$  with uniformly  $(0, 1)$  distributed random for real and imaginary part.
  - 4:  $\mathbf{R}^{\text{old}} = \mathbf{R}$ ,  $\mathbf{Z}^{\text{old}} = \mathbf{Z}$
  - 5: **while**  $\|\mathbf{S} - \mathbf{S}^{\text{old}}\|_F < \epsilon_{\min}$  **do**
  - 6:  $\mathbf{S} = \begin{bmatrix} \Gamma_\Omega \mathbf{R}^{\text{old}} \Gamma_\Omega^T & \tilde{\mathbf{R}}_\Omega \\ \tilde{\mathbf{R}}_\Omega & \mathbf{Z}^{\text{old}} \end{bmatrix}$
  - 7: PSD projection:  $\mathbf{S} = P_{\mathcal{P}}(\mathbf{S})$  (18)
  - 8:  $\mathbf{R} = \Gamma_\Omega^\dagger \mathbf{S} (1 : M, 1 : M) (\Gamma_\Omega^\dagger)^T$  (15)
  - 9: Rank-constraint projection:  $\mathbf{R} = P_{\mathcal{R}}(\mathbf{R})$  (19)
  - 10: Toeplitz projection:  $\mathbf{R} = P_{\mathcal{T}}(\mathbf{R})$  (16)
  - 11:  $\mathbf{S} (1 : M, 1 : M) = \Gamma_\Omega \mathbf{R} \Gamma_\Omega^T$
  - 12:  $\mathbf{R}^{\text{old}} = \mathbf{R}$ ,  $\mathbf{Z}^{\text{old}} = \mathbf{S} (M+1 : 2M, M+1 : 2M)$
  - 13: **end while**
  - 14: Output:  $\mathbf{R}$
- 

##### 4.4. Alternating projections

Initialized parameters  $\mathbf{R}$  and  $\mathbf{Z}$  form  $\mathbf{S}$ , which is PSD, i.e.,  $\mathbf{S} = P_{\mathcal{P}}(\mathbf{S})$  (18).  $\mathbf{R}$  is obtained from  $\mathbf{S}$ ,  $\mathbf{R} = \Gamma_\Omega^\dagger \mathbf{S} (1 : M, 1 : M) (\Gamma_\Omega^\dagger)^T$  (15), and the projection  $P_{\mathcal{R}}(\mathbf{R})$  (19) is carried out to make  $\mathbf{R}$  be  $K$ -rank. The projection  $P_{\mathcal{T}}(\mathbf{R})$  (16) is followed for a Toeplitz structure. Submatrix  $\Gamma_\Omega \mathbf{R} \Gamma_\Omega^T$  is implemented in  $\mathbf{S}$ . AP-GLS iterates the projections until it converges to a solution. AP-GLS is summarized in Algorithm 1.

##### 4.5. DOA retrieval

DOAs  $\theta_k$ ,  $k = 1, \dots, K$ , are recovered by the Vandermonde decomposition (5) for the rank- $K$  PSD Toeplitz matrix  $\mathbf{R}$ . [5, 6, 8] The Vandermonde decomposition is computed efficiently via root-MUSIC [26]:

1. Perform the eigen-decomposition in signal- and noise-subspace, i.e.,  $\mathbf{R} = \mathbf{U}_S \mathbf{\Lambda}_S \mathbf{U}_S^H + \mathbf{U}_N \mathbf{\Lambda}_N \mathbf{U}_N^H$ .
2. Compute the root-MUSIC polynomial  $\mathcal{Q}(z) = \mathbf{a}^T (1/z) \mathbf{U}_N \mathbf{U}_N^H \mathbf{a}(z)$ , where  $\mathbf{a} = [1, z, \dots, z^{M-1}]^T$  and  $z = e^{-j(2\pi/\lambda)d \sin \theta}$ .
3. Find the roots of  $\mathcal{Q}(z)$  and choose the  $K$  roots that are inside the unit circle and closest to the unit circle, i.e.,  $\hat{z}_i$ ,  $i = 1, \dots, K$ .
4. DOA estimates are recovered, i.e.,  $\hat{\theta}_i = -\sin^{-1}(\frac{\lambda \angle \hat{z}_i}{2\pi d})$ ,  $i = 1, \dots, K$ .

## 5. SIMULATION RESULTS

We consider a ULA with  $M = 16$  elements, half-wavelength spacing, and a co-prime array with  $M = 8$  elements with  $M_1 = 5$  and  $M_2 = 2$  (elements 1, 3, 5, 6, 7, 9, 11, 16).

The signal-to-noise ratio (SNR) is defined,  $\text{SNR} = 10 \log_{10} [\mathbb{E}\{\|\mathbf{A}\mathbf{s}_l\|_2^2\} / \mathbb{E}\{\|\mathbf{e}_l\|_2^2\}]$ , where  $\mathbf{s}_l \in \mathbb{C}^K$  and  $\mathbf{e}_l \in \mathbb{C}^M$ ,  $l = 1, \dots, L$ , are the source amplitude and the measurement noise for the  $l$ th snapshot. The root mean squared error

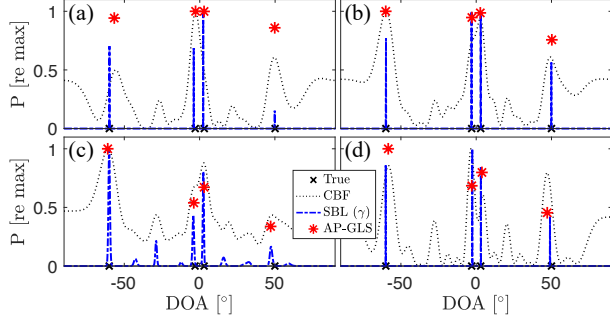


**Fig. 1.** DOA estimation from  $L$  snapshots for  $K = 4$  sources with an  $M = 8$  co-prime array. CBF, SBL, and AP-GLS for (a) incoherent sources with SNR 20 dB and one snapshot,  $L = 1$ , (b) SNR 20 dB and  $L = 20$ , (c) SNR 0 dB and  $L = 20$ , and (d) for coherent sources with SNR 20 dB and  $L = 20$ .

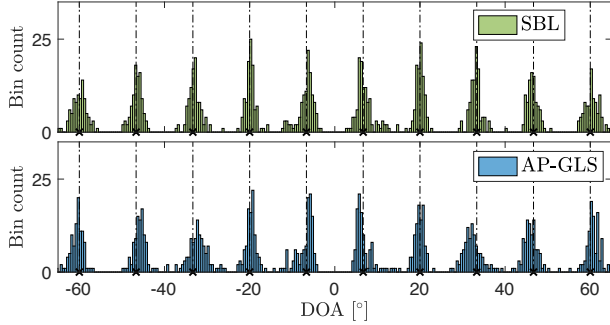


**Fig. 2.** Histogram of the estimated DOAs of SBL and AP-GLS for  $K = 10$  sources with an  $M = 8$  co-prime array for 100 trials. ( $M < K$ )

(RMSE) is,  $\text{RMSE} = \sqrt{\mathbb{E} \left[ \frac{1}{K} \sum_{k=1}^K (\hat{\theta}_k - \theta_k)^2 \right]}$ , where  $\hat{\theta}_k$  and  $\theta_k$  represent estimated and true DOA of the  $k$ th source.

We consider an  $M = 8$  co-prime array and  $K = 4$  stationary sources at DOAs  $[-60, -3, 3, 50]^\circ$  with snapshot-varying magnitudes  $[12, 20]$  dB in four scenarios, see Fig. 1. Conventional beamforming (CBF), SBL [28, 29], and AP-GLS are compared. CBF cannot distinguish close two DOAs  $[-3, 3]^\circ$ . AP-GLS solves the single snapshot case and resolve the close arrivals. We also consider the DOA performance with a coherent sources due to multipath arrivals. AP-GLS still shows accurate DOAs.

Co-prime arrays can estimate more sources than the number of sensors, see Fig. 2. We consider the same co-prime array and  $K = 10$  stationary sources uniformly distributed in  $[-60, 60]^\circ$ , with  $L = 20$  and SNR 20 dB. The histogram shows the distribution of the DOA estimates of AP-GLS.

The DOA performance is evaluated with the RMSE versus SNR, see Fig. 3. RMSE larger than 10 times the median is outlier and eliminated. We consider  $K = 4$  sources, same as in Fig. 1 but with equal strengths. Cramér-Rao bound (CRB) [32], MUSIC and MUSIC with co-array interpolation

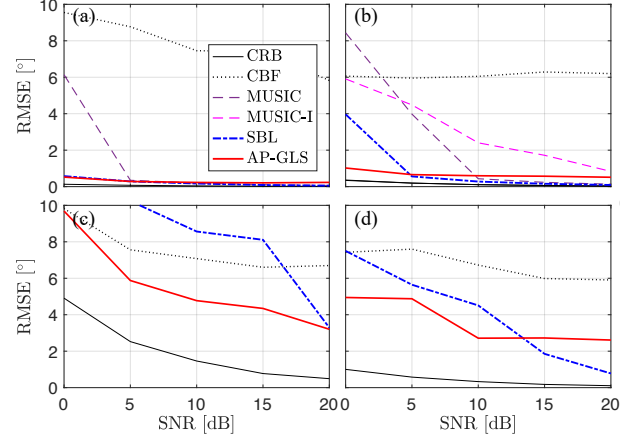


**Fig. 3.** RMSE  $[\circ]$  comparison versus SNR. Each RMSE is averaged over 100 trials.  $K = 4$  incoherent sources for (a) an  $M = 16$  ULA with  $L = 20$ , (b) an  $M = 8$  co-prime array with  $L = 20$ , (c)  $L = 1$ , and (d) coherent sources for a co-prime array with  $L = 20$ .

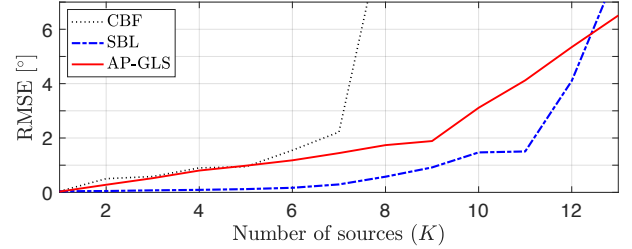


**Fig. 4.** RMSE  $[\circ]$  comparison versus  $K$ . Each RMSE is averaged over 100 trials. An  $M = 8$  co-prime array is used with  $L = 20$  and SNR 20 dB.

(MUSIC-I) [33] are also compared. Compared to full ULA cases, AP-GLS has a bounded error even with high SNR, which is come from the fact that  $\mathbf{R}$  is recovered from its sub-matrix  $\mathbf{\Gamma}_\Omega \mathbf{R} \mathbf{\Gamma}_\Omega^T$ .

The DOA performance is evaluated with the RMSE versus number of sources  $K$ , see Fig. 4. We consider the same co-prime array and for each case,  $K$  equal strength sources are generated randomly in  $[-65, 65]^\circ$ , with  $L = 20$  and SNR 20 dB. AP-GLS has higher estimation accuracy than CBF and estimating more sources than the number of sensors.

## 6. CONCLUSION

We introduced alternating projections based gridless sparse iterative covariance-based estimation for direction-of-arrival estimation that is gridless and promotes sparse solutions. Numerical evaluations indicated that the proposed method shows a favorable performance even with single-snapshot data and coherent arrivals. For co-prime array data, the proposed algorithm resolved more sources than the number of sensors.

## 7. REFERENCES

- [1] D. Malioutov, M. Cetin, and A. S. Willsky, "A sparse signal reconstruction perspective for source localization with sensor arrays," *IEEE Trans. Signal Process.*, vol. 53, no. 8, pp. 3010–3022, Aug 2005.
- [2] P. Gerstoft, A. Xenaki, and C.F. Mecklenbräuker, "Multiple and single snapshot compressive beamforming," *J. Acoust. Soc. Am.*, vol. 138, no. 4, pp. 2003–2014, 2015.
- [3] A. Xenaki and P. Gerstoft, "Grid-free compressive beamforming," *J. Acoust. Soc. Am.*, vol. 137, no. 4, pp. 1923–1935, 2015.
- [4] Y. Park, Y. Choo, and W. Seong, "Multiple snapshot grid free compressive beamforming," *J. Acoust. Soc. Am.*, vol. 143, no. 6, pp. 3849–3859, 2018.
- [5] Z. Yang, J. Li, P. Stoica, and L. Xie, "Sparse methods for direction-of-arrival estimation," in *Academic Press Library in Signal Processing: Array, Radar and Communications Engineering*, vol. 7, chapter 11, pp. 509 – 581. Academic Press, 2018.
- [6] G. Tang, B. N. Bhaskar, P. Shah, and B. Recht, "Compressed sensing off the grid," *IEEE Trans. Inf. Theory*, vol. 59, no. 11, pp. 7465–7490, 2013.
- [7] Y. Chi, L. L. Scharf, A. Pezeshki, and A. R. Calderbank, "Sensitivity to basis mismatch in compressed sensing," *IEEE Trans. Signal Process.*, vol. 59, no. 5, pp. 2182–2195, 2011.
- [8] Y. Chi and M. Ferreira Da Costa, "Harnessing sparsity over the continuum: Atomic norm minimization for superresolution," *IEEE Signal Process. Mag.*, vol. 37, no. 2, pp. 39–57, 2020.
- [9] Y. Wang, Y. Zhang, Z. Tian, G. Leus, and G. Zhang, "Super-resolution channel estimation for arbitrary arrays in hybrid millimeter-wave massive MIMO systems," *IEEE J. Sel. Topics Signal Process.*, vol. 13, no. 5, pp. 947–960, Sep. 2019.
- [10] A. G. Raj and J. H. McClellan, "Super-resolution DOA estimation for arbitrary array geometries using a single noisy snapshot," in *Proc. IEEE ICASSP*, 2019, pp. 4145–4149.
- [11] S. Semper, F. Roemer, T. Hotz, and G. Del Galdo, "Grid-free direction-of-arrival estimation with compressed sensing and arbitrary antenna arrays," in *Proc. IEEE ICASSP*, 2018, pp. 3251–3255.
- [12] Z. Yang, L. Xie, and C. Zhang, "A discretization-free sparse and parametric approach for linear array signal processing," *IEEE Trans. Signal Process.*, vol. 62, no. 19, pp. 4959–4973, 2014.
- [13] P. Stoica, P. Babu, and J. Li, "SPICE: A sparse covariance-based estimation method for array processing," *IEEE Trans. Signal Process.*, vol. 59, no. 2, pp. 629–638, 2011.
- [14] Z. Zhu and W. B. Wakin, "On the asymptotic equivalence of circulant and Toeplitz matrices," *IEEE Trans. Inf. Theory*, vol. 63, no. 5, pp. 2975–2992, 2017.
- [15] D. Romero and G. Leus, "Wideband spectrum sensing from compressed measurements using spectral prior information," *IEEE Trans. Signal Process.*, vol. 61, no. 24, pp. 6232–6246, 2013.
- [16] S. Boyd and L. Vandenberghe, *Convex optimization*, Cambridge university press, Cambridge, U.K., 2004.
- [17] J. Dattorro, *Convex optimization & Euclidean distance geometry*, Meboo Publishing USA, Palo Alto, CA, USA, 2010.
- [18] H. Q. Cai, J.-F. Cai, and K. Wei, "Accelerated alternating projections for robust principal component analysis," *J. Mach. Learn. Res.*, vol. 20, no. 1, pp. 685–717, 2019.
- [19] X. Jiang, Z. Zhong, X. Liu, and H. C. So, "Robust matrix completion via alternating projection," *IEEE Signal Process. Lett.*, vol. 24, no. 5, pp. 579–583, 2017.
- [20] A. S. Lewis and J. Malick, "Alternating projections on manifolds," *Math. Oper. Res.*, vol. 33, no. 1, pp. 216–234, 2008.
- [21] P. Netrapalli, U. N. Niranjan, S. Sanghavi, A. Anandkumar, and P. Jain, "Non-convex robust PCA," in *Proc. NIPS*, 2014, pp. 1107–1115.
- [22] M. Cho, J. Cai, S. Liu, Y. C. Eldar, and W. Xu, "Fast alternating projected gradient descent algorithms for recovering spectrally sparse signals," in *Proc. IEEE ICASSP*, 2016, pp. 4638–4642.
- [23] L. Condat and A. Hirabayashi, "Cadzow denoising upgraded: A new projection method for the recovery of Dirac pulses from noisy linear measurements," *Sampl. Theory Signal Image Process.*, vol. 14, no. 1, pp. 17–47, 2015.
- [24] X. Wu, W. Zhu, and J. Yan, "A Toeplitz covariance matrix reconstruction approach for direction-of-arrival estimation," *IEEE Trans. Veh.*, vol. 66, no. 9, pp. 8223–8237, Sep. 2017.
- [25] M. Wagner, P. Gerstoft, and Y. Park, "Gridless DOA estimation via alternating projections," in *Proc. IEEE ICASSP*, 2019, pp. 4215–4219.
- [26] M. Wagner, Y. Park, and P. Gerstoft, "Gridless DOA estimation and root-MUSIC for non-uniform arrays," *arXiv preprint arXiv:2003.04457*, 2020.
- [27] P. P. Vaidyanathan and P. Pal, "Sparse sensing with co-prime samplers and arrays," *IEEE Trans. Signal Process.*, vol. 59, no. 2, pp. 573–586, 2010.
- [28] S. Nannuru, A. Koochakzadeh, K. L. Gemba, P. Pal, and P. Gerstoft, "Sparse Bayesian learning for beamforming using sparse linear arrays," *J. Acoust. Soc. Am.*, vol. 144, no. 5, pp. 2719–2729, 2018.
- [29] S. Nannuru, P. Gerstoft, A. Koochakzadeh, and P. Pal, "Sparse Bayesian learning for DOA estimation using co-prime and nested arrays," in *Proc. 10th IEEE SAM*, 2018, pp. 519–523.
- [30] C. Steffens, M. Pesavento, and M. E. Pfetsch, "A compact formulation for the  $\ell_{2,1}$  mixed-norm minimization problem," *IEEE Trans. Signal Process.*, vol. 66, no. 6, pp. 1483–1497, 2018.
- [31] M. G. Eberle and M. C. Maciel, "Finding the closest Toeplitz matrix," *Comput. Appl. Math.*, vol. 22, no. 1, pp. 1–18, 2003.
- [32] P. Stoica and A. Nehorai, "Music, maximum likelihood, and Cramér-Rao bound," *IEEE Trans. Acoust., Speech, Signal Process.*, vol. 37, no. 5, pp. 720–741, 1989.
- [33] C. Liu and P. P. Vaidyanathan, "Remarks on the spatial smoothing step in coarray MUSIC," *IEEE Signal Process. Lett.*, vol. 22, no. 9, pp. 1438–1442, 2015.